23rd ABCM International Congress of Mechanical Engineering
December 6-11, 2015, Rio de Janeiro, RJ, Brazil

EVALUATION OF FRACTURE ENERGY USING THE DIGITAL IMAGE CORRELATION

Ayrton Hugo de Andrade e Santos
Departamento de Engenharia Civil - Instituto Politécnico - Pontifícia Universidade Católica de Minas Gerais. End.: Av. Dom José Gaspar, 500, Prédio 13, Sala 101 - Coração Eucarístico - Belo Horizonte/MG - CEP 30535-901
ayrtonhugo@yahoo.com.br

Gabriel de Oliveira Ribeiro
Roque Luiz da Silva Pitangueira
Departamento de Engenharia de Estruturas - Escola de Engenharia - Universidade Federal de Minas Gerais. End.: Av. Antônio Carlos, 6627 - Pampulha, sala 4125 - Cep 31270-901, Belo Horizonte/MG
gabriel@dees.ufmg.br; roque@dees.ufmg.br

The fracture energy is defined as amount of energy required to create one unit of area of a crack of an infinite specimen size and can be assessed in terms of the stable load-deflection curve. These curves may be obtained in the traditional way using displacement transducers or with alternative methods such as digital images. In this paper an experimental evaluation of the fracture energy in granular materials is performed applying Digital Image Correlation (DIC) technique to measure displacements on the surface of beams. Three point bending tests were performed on three different size concrete beams (50 mm, 100 mm and 200 mm) with a notch at the midspan. The results allow a better understanding of the fracture energy increased with increasing size concrete beams and demonstrate the efficiency of Digital Image Correlation to obtain measures of displacements.

Keywords: *Fracture Energy; Digital Image Correlation; Experimental Analysis.*

1. INTRODUCTION

Fracture toughness of granular materials like concrete can not be analyzed in dissociation of the size effect in structures. The size effect in concrete fracture , was first reported in 1961 by Kaplan (1961) and has attracted the attention of several researchers (Higgins and Bailey (1976), Mindess (1984), Bazant (1984), Wittmann (1992) Duan (2003) in recent decades, particularly after the Size Effect Law (SEL) by Bazant (1984,1987) and specific fracture energy G_f proposed by RILEM. (1985).

Experimental studies have shown that, while the strenght of concrete decreases with the increasing of the size of the specimen (which can not be adequately described by the Weibull's statistical fracture theory), the fracture energy, which is defined as the rate of energy required for the growth of the crack of an infinite size specimen, increases with the increase in the size of the specimen.

Specifically for concrete, the flaw is usually accompanied by cracks that usually begin in areas that are subjected to tension stresses. The emergence of these cracks and their propagation are the result of physical processes that are usually explained by energy conservation laws. In many of these theories concrete is considered a homogeneous material, however, the effect of the manufacturing process, the shape of the constituents and the size of elements influence the cracking process.

In order to evaluate the energy which is required for stable crack propagation, the consolidated test is the beams with notches subjected to three point bending. In this test, the parts are loaded at a constant displacement rate until its rupture, plotting load versus displacement curves. The area under the curve is the fracture energy of the material. These curves may be obtained in the traditional way using displacement transducers or alternative methods as digital image correlation.

That said, this study aims to experimentally quantify the fracture energy in granular materials (concrete) using as measurement tool the digital image correlation, demonstrating the efficiency of the digital image correlation in obtaining displacement measures.

2. DIGITAL IMAGE CORRELATION TECHNIQUE

Digital image correlation (DIC) is an optical method to visualize displacement fields by successive post-processing of captured images at a constant frequency, as explained by Skarzynski et al. (2011).

This technique uses textural patterns, natural or artificial, as information carriers. Displacement patterns can be obtained by combining the captured image surfaces before and after the deformation or displacement using a function of adequate correlation (Sutton et al. (2000)).

The images are captured by high-precision digital cameras with sensors. The sensors of these cameras are composed of small, photo-sensitive elements, called pixels. When an image is captured, each pixel represents three numbers (color components Y, Cb, and Cr) at the proportion of the amount of light reflected by the object being photographed. The Y, Cb, and Cr indexes represent luminosity or brightness, blue tonality, and red tonality, respectively. The digital image correlation system should be able to interpret different light intensities and record grayscale patterns for each pixel such that each point is unique.

To use the digital image correlation technique, the system should have at least three functions, as indicated by Skarzynski et al. (2011), which are (i) image intensity field, (ii) correlation function, and (iii) interpolation function.

The image intensity field attributes a scalar value to each point of the image plane that represents the light intensity (Y component) of the corresponding point in the physical space. The image intensity field also indicates the shades of grey that represent the point, which can vary numerically between 0 (black) and 255 (white) for an 8-bit image.

In the digital image, the area of interest should be selected, and small subsets, called patterns, should be chosen. In Fig. 1, four patterns are selected in the first image, and the first pattern is observed in the second image. If the displacements of these patterns between two sequential images are too small, their Cartesian positions are considered to have been maintained. The strain pattern is detected by comparing two consecutive images, which are captured by a digital camera that is maintained at a fixed position with its axis oriented perpendicular to the beam's surface plane, as indicated by Pan et al. (2009) (Fig. 2).

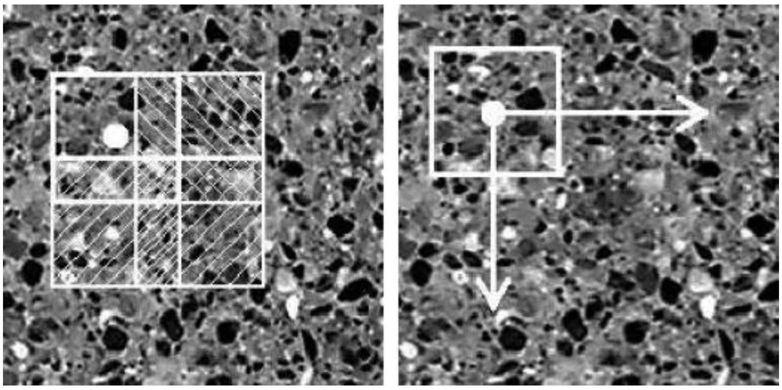

Figure 1. Two successive digital images of an area of interest and respective pixel subsets, which indicates patterns to be observed (Skarzynski et al. (2011))

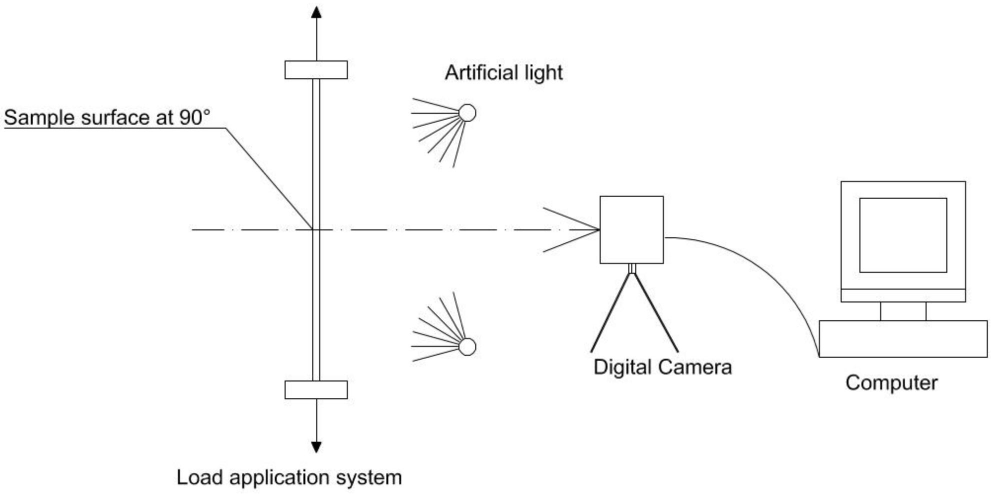

Figure 2. Digital image capture system (modified) (Pan et al. (2009))

A local displacement vector is obtained for each pattern (Fig. 1) using a correlation function between two consecutive light intensity distributions (Y component) in two digital images. The function calculates possible displacements and correlates all grey values from the first image with all of the grey values from the second image. This displacement vector is adjusted using an interpolation function.

In digital cameras, charged coupled devices operate in the Y-Cb-Cr color space as opposed to the R-G-B color space (R is red, G is green, B is blue). Image storage is preceded by conversion of the R-G-B to the Y-Cb-Cr color space according to Norm ISO/TC42N 4378(1998), as indicated in Eq. (1).

$$\begin{aligned} Y &= 0.2989R + 0.5866G + 0.1145B; \\ C_b &= 128 - 0.168736R - 0.331264G + 0.5B; \\ C_r &= 128 + 0.5R - 0.418688G - 0.081312B. \end{aligned} \tag{1}$$

The precision of the digital image correlation technique is strongly dependent on the size of the pattern selected and on its quality. The pattern spot should contain 4 to 10 pixels on the surface of the specimen, as indicated by Skarzynski et al. (2011).

3. PROGRAM EXPERIMENTAL

The experimental program consisted of laboratory tests using beams subjected to flexural bending at three points performed in concrete specimens of three different sizes. Tab. 1 presents the nominal dimensions of the tested beams according to the scheme represented in Fig. 3.

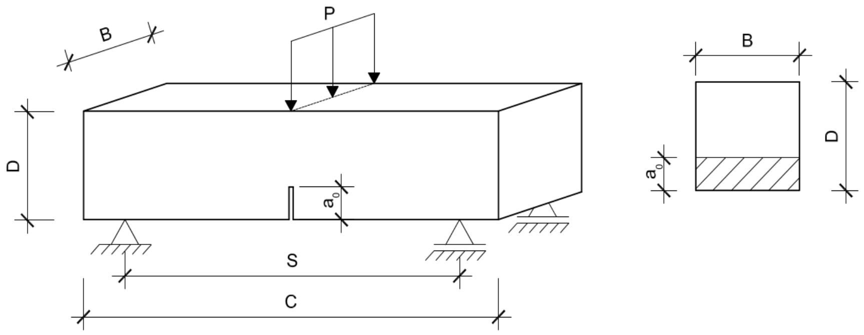

Figure 3. Diagram of the three-point bending test on a concrete beam

Table 1 - Beam dimensions.

Beam	Total Span – C (mm)	Effective Span – S (mm)	Thickness – B (mm)	Height – D (mm)	Notch – a_0 (mm)
B1	260	200	80	50	20
B2	460	400	80	100	40
B3	860	800	80	200	80

The specimens were composed of a rectangular cross-section (B x D) with a fixed width of 80 mm and an effective span (S) equal to four times the section height D. The notch at the mid-section of the span (a_0) was maintained at 40% of the beam height. The notch on the underside of each specimen was wet-cut using a diamond cutting disk with a thickness of approximately 2 mm. The Fig. 4 shown the specimens.

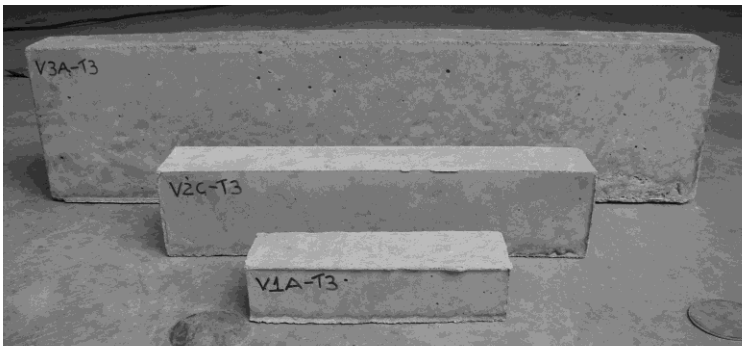

Figure 4. Different size concrete beams

The concrete used was made from a Portland CPV-ARI cement mixture; the fine aggregates had a fineness modulus equal to 2.3 mm, and the coarse aggregates had a maximum diameter of 25.0 mm.

To determine the mechanical parameters of the compressive strength, tensile strength, and static elastic modulus of concrete, an EMIC PC 200 servo-hydraulic machine was used following the recommendations of norms NBR 5739 (2007), NBR 8522(2008), and NBR 7222(2011), respectively. The cylindrical specimens measured 100 mm in diameter and 200 mm in length. Tab. 2 presents the values of these mechanical parameters.

Table 2 - Mechanical parameters of concrete.

Parameter	Mean (MPa)	Standard Deviation (MPa)	Coeff. of Variation (%)
Compressive Strength	24.3	1.13	5.03
Elastic Modulus	35882	2025	6.56
Tensile Strength	2.39	0.14	2.80

To apply the load, a plane frame with an EMIC DL 30000 servo-hydraulic machine with a 300-kN load capacity was used. A 50-kN load cell was coupled to this machine for compliance of the load-displacement results in the data acquisition system. The beam displacement control was induced by a vertical displacement "v" imposed on the half span of the beam at a rate of 0.009 mm/min.

Before the test, the surfaces of the concrete beams were polished and then grid-marked for better monitoring of the standards. The images were captured by a high-resolution USB microscope with a 2.0 megapixel image sensor and video resolution capture of 1280 x 960. The image capture rate was set at 5 frames per second, which was recorded in an AVI format, and the light was generated by LED lamps from the microscope itself. This equipment along with the digital image processing software developed in a LabView platform, was used to analyze the translation and rotation movements of the monitoring standards; thus, the relative displacements could be determined. The captured images were synchronized with the measurements of the test machine. Test equipment and USB microscope 800x are shown in Fig 5 for testing the beam B3.

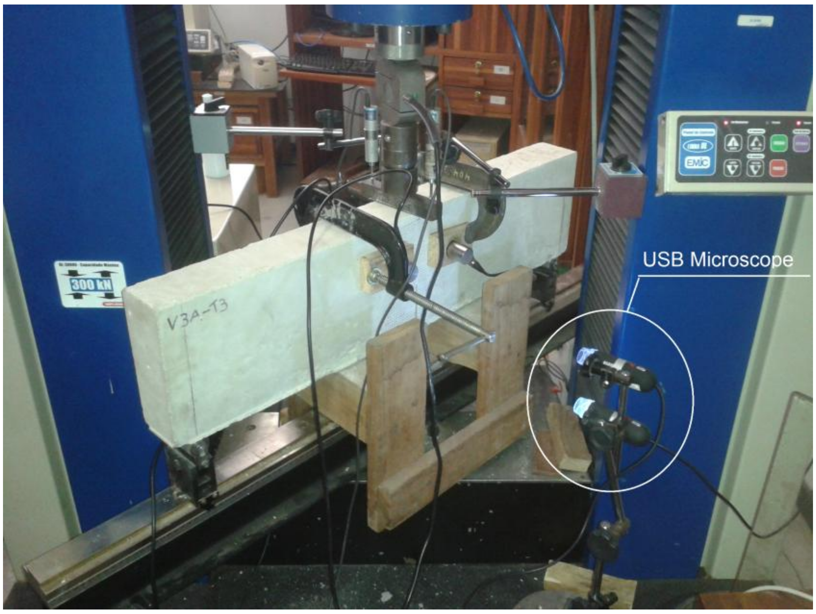

Figure 5. EMIC DL 30000 servo-hydraulic machine and USB microscope 800x

4. RESULTS AND DISCUSSION

For each beam size presented in Tab. 1, three specimens were tested. The load versus vertical displacement curves in the mid-span for the three tested sizes are grouped in Fig.6 (a),(b),(c), creating the experimental spectrum. The vertical displacement was measured at the underside of the beam.

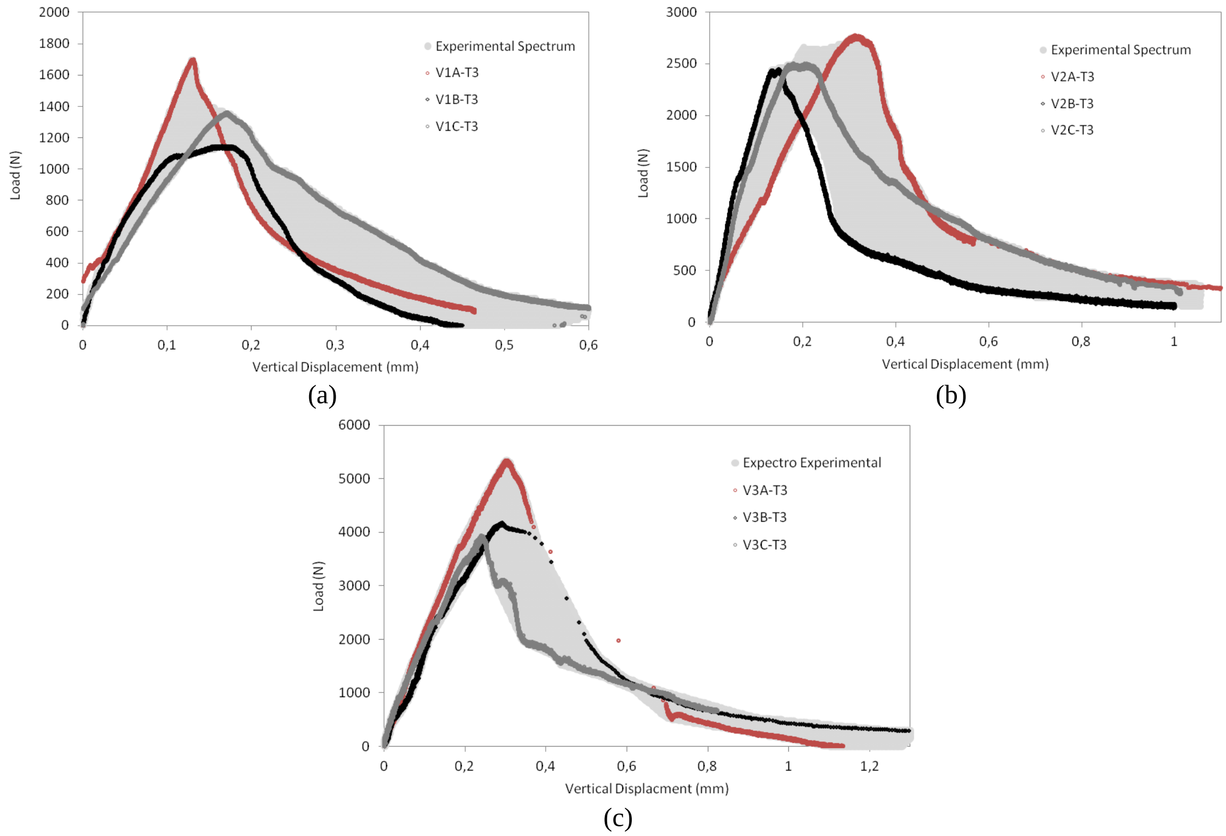

Figure 6. Load x displacement curves and experimental spectrum

With reference to the experimental spectrum has created an average curve for the three sizes of the beams, with three medium grouped on one graph, as shown in Fig. 7

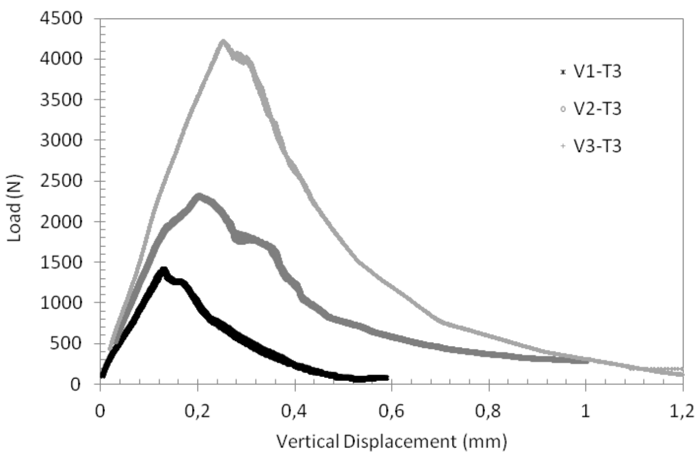

Figure 7. Load x displacement curves avarage for three beam sizes

After calculating the areas under the load-displacement curves presented in Fig. 7, the values of the work were obtained, which were equal to 312.4 Nmm, 947.68 Nmm, and 2147.54 Nmm for beam sizes B1, B2, and B3, respectively. Using these values and Eq. 1, the respective fracture energies (G_F) were obtained, as presented in Tab. 3. An increase in the fracture energy with increases in the specimen size was observed. This fact was also observed by Nallathambi et al.(1994) apud Karihaloo (1995), Gettu et al. (1984), and Hillerborg 1995 after performing more than 700 three-point flexural tests in beams. The fracture energy values found using DIC varied between 130.17 and 223.7 N/m.

These results are extremely similar to those found by Nallathambi et al. (1994) apud Karihaloo (1995), who determined using conventional methods that G_F varies between 90 N/m and 250 N/m for samples with spans, heights, and notches equivalent to those presented in this study.

Table 3 - Fracture energy G_F

Beam	Height – D (mm)	Area under the curve (N x mm)	Energy - G_F (N/m)
B1	50	312.40	130.17
B2	100	805.53	167.82
B3	200	2147.54	223.70

The reason why G_F varies with specimen size is due to the hypothesis proposed in Eq. 1, where all work performed by the external load is completely reversed to the stable propagation of the crack. Figure 8 shows the variation in GF with the height of the specimens (D).

$$Energy = \frac{Area\ under\ load\ \text{-}\ displacement\ curve}{B \cdot (D - a_0)} \tag{1}$$

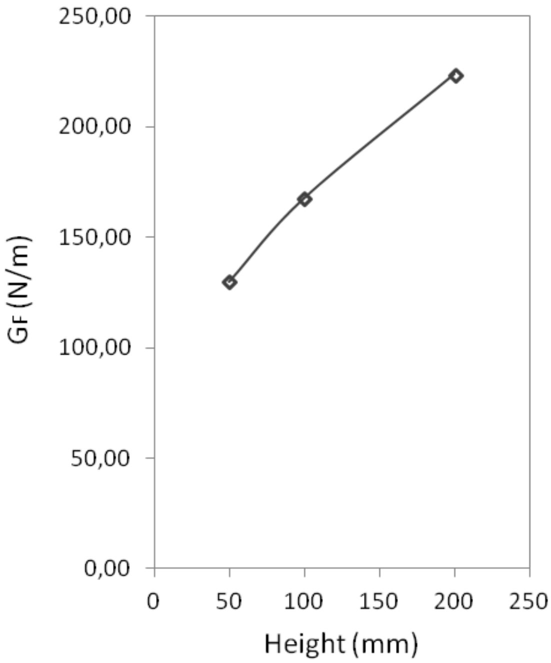

Figure 8. Variation in fracture energy (*GF*) with specimen height *(D)*

Figure 7 also indicates that the longer the beam, the steeper the slope of the descending section of the trajectory is, which is a direct consequence of the size effect on structural ductility.

5. CONCLUSION

In this study, an experimental investigation of fracture energy in granular materials using the digital image correlation technique was performed.

DIC was found to be an effective technique to determine displacement fields on concrete surfaces with the advantage of not requiring physical contact with the specimen's surface.

This technique allowed observing the fracture energy behavior with changing the size of the specimen. and verified an increase in the fracture energy with increases in the specimen size.

6. REFERENCES

Skarzynski, Ł.; Syroka, E and Tejchman, J., 2011. "Measurements and Calculations of the Width of the Fracture Process Zones on the Surface of Notched Concrete Beams". *Strain*, v. 47, p. 319-332.

Sutton, M. A.; McNeill, S. R.; Helm, J. D. and Chao, Y. J., 2000. "Advances in two-dimensional and three-dimensional computer vision". *Top. Appl Phys*, v. 77, p.323-372.

Pan, B., Quian, K., Xie, H. and Asundi, A., 2009. “Two-dimensional digital image correlation for in-plane displacement and strain measurement: a review.” *Measurement Science and Technology*, v. 20, p. 1-17.

ISO/TC42N 4378, 1998. "Photography-Electronic Still Picture Imaging-Removable Memory-Part 2:" *Image Data Format-TIFF/EP*, Nov. 25.

Kaplan, M.F., 1961 "Crack propagation and the fracture of concrete", *ACIJ*. 58, 591-610.

Higgins, D.D. and Bailey, J.E.,1976. "Fracture measurements on cement paste",*J. Mater. Sci*. v.11 p.1995-2003.

Mindess, S.,1984, "The effect of specimen size on the fracture energy of concrete", *Cem. Concr. Res*. v.14 p.431-436.

Bazant, Z.P.,1984."Size effect in blunt fracture: concrete, rock, metal", *J. Eng. Mech*. ASCE v.110(4); p.518-535.

Bazant, Z.P. and Pfeiffer, P.A.,1987 "Determination of fracture energy from size effect and brittleness number", *ACI Mater. Journal*, .v.84 p.463-480.

RILEM TC 50-FMC, 1985 "Determination of the fracture energy of mortar and concrete by means of three-point bend tests on notched beams", *Materials. Structures*. v.18 p. 287-290.

Wittmann, F.H., 1992."Fracture process zone and fracture energy', in 'Fracture Mechanics of Concrete Structures", Proc. FRAMCOS-1, Breackenridge, Colorado, USA, 1-5, *ed. Z.P.Bakant (Elsevier Applied Science)* 391-403.

Duan, K, Hu, X.-Z.and and Wittmann, F. H, 2003."Size Effect on fracture resistance and fracture energy of concrete", *Materials and Structures* v.36, p.74-80

ABNT, 2007. Concreto - Ensaios de compressão de corpos-de-prova cilíndricos – Métodos de ensaio. *NBR 5739*, Rio de Janeiro.

ABNT, 2008. Concreto - Determinação do módulo estático de elasticidade à compressão. *NBR 8522*, Rio de Janeiro.

ABNT, 2011. Concreto e argamassa – Determinação da resistência à tração por compressão diametral de corpos-de-prova cilíndricos. *NBR 7222*, Rio de Janeiro.

Karihallo, B. L.,1995; Fracture Mechanics and Structural Concrete. *Longman Scientific & Technical*, New York

Nallathambi, P., Karihallo, B. L and Heaton, 1994, B.S. Effect of specimen and crack size, water/cement ratio and coarse aggregate texture upon fracture toughness of concrete, *Mag Concr Res*, vol. 36, p.227-236

Gettu, T; Bazant, Z, P. and Karr, M.E; 1984 Fracture properties and brittleness of high strength concrete, *ACI Mater J.* vol. 87, p.608-618

Hillerborg, A.,1995 Influence of beam size on concrete fracture energy determined according to a draft RILEM recommendation, *Report TVBM-3201, Div Bldg Mater Lund Inst Tech, Sweden*.

7. RESPONSIBILITY NOTICE

The authors are the only responsible for the printed material included in this paper.